

PACS 78.40.Ha, 77.80.Bh

Structural, electrical and optical investigations of $\text{Cu}_6\text{PS}_5\text{Br}$ -based thin film deposited by HiTUS technique

I.P. Studenyak¹, M.M. Kutsyk¹, V.I. Studenyak¹, A.V. Bendak¹, V.Yu. Izai¹, P. Kúš², M. Mikula^{2*}

¹*Uzhhorod National University, Faculty of Physics,*

3 Narodna Sq., 88000 Uzhhorod, Ukraine

²*Comenius University, Faculty of Mathematics, Physics and Informatics,*

Mlynska dolina, 84248 Bratislava, Slovakia,

E-mail: studenyak@dr.com

Abstract. $\text{Cu}_{6.35}\text{P}_{1.77}\text{S}_{4.72}\text{Br}_{0.15}$ thin film was obtained using the high target utilization sputtering onto *c*-cut sapphire substrates. X-ray diffraction studies show the film to be amorphous with some crystalline inclusions. SEM investigations indicate formation of periodical “forest-like” quasi-two-dimensional pillared structure. Electrical conductivity of $\text{Cu}_{6.35}\text{P}_{1.77}\text{S}_{4.72}\text{Br}_{0.15}$ thin film was measured in the temperature interval 4.5...300 K, three regions with different activation energy were revealed. Optical constants were obtained using the technique of spectroscopic ellipsometry and used for calculation of optical absorption spectrum. Optical absorption edge has an exponential form, the Urbach energy shows the significant disordering in $\text{Cu}_{6.35}\text{P}_{1.77}\text{S}_{4.72}\text{Br}_{0.15}$ thin film.

Keywords: thin film, high target utilization sputtering, X-ray diffraction, electrical conductivity, optical constants.

Manuscript received 29.04.16; revised version received 12.07.16; accepted for publication 13.09.16; published online 04.10.16.

1. Introduction

$\text{Cu}_6\text{PS}_5\text{Br}$ crystals belong to the argyrodite family and are well known as superionic conductors [1]. They possess high ionic conductivity and low activation energy, which makes them promising for applications as electrochemical energy sources [2]. The efficient ion transport in $\text{Cu}_6\text{PS}_5\text{Br}$ crystal is explained by the specific structure that facilitates fast ion transport [3]. At room temperature, $\text{Cu}_6\text{PS}_5\text{Br}$ crystals belong to the cubic syngony ($F\bar{4}3m$ space group), while at low temperatures two phase transitions (PTs) occur: the ferroelastic one at $T_{II} = (268 \pm 2)$ K and superionic one at $T_I = (166 \dots 180)$ K [4]. Below the ferroelastic PT temperature $\text{Cu}_6\text{PS}_5\text{Br}$ crystals belong to the monoclinic syngony (*Cc* space

group), and the superionic PT reveals the features of an isostructural transformation [4]. Anomalous behaviour of dielectric, calorimetric and acoustic properties has been revealed in the range of the phase transitions [5-8].

Optical studies in $\text{Cu}_6\text{PS}_5\text{Br}$ crystal have shown that exciton absorption bands can be observed at $T < T_I$ [9]. In the vicinity of the superionic PT, the bands undergo considerable changes, which are caused by dynamic structural disordering of copper cation sublattice. At $T > T_I$, at the absorption edge the exponential parts appear, being described by the Urbach rule [9]. The optical absorption processes in $\text{Cu}_6\text{PS}_5\text{Br}$ crystal is well explained in the framework of the known Dow-Redfield model, the nature of electron-phonon interaction remaining unchanged at PT from one

crystalline structure to another. The slope of the exponential Urbach edge of $\text{Cu}_6\text{PS}_5\text{Br}$ crystal is determined by both temperature and structural disordering.

The investigations of the thin films based on $\text{Cu}_6\text{PS}_5\text{Br}$ superionic conductors only begin. Thus, in this paper the structural, electrical and optical properties of $\text{Cu}_6\text{PS}_5\text{Br}$ -based thin film are studied. Besides, the comparative analysis of optical parameters in single crystal and thin film is performed.

2. Experimental

$\text{Cu}_6\text{PS}_5\text{Br}$ -based thin films were deposited on *c*-cut sapphire substrates at room temperature by means of high target utilization sputtering (PQL HiTUS S500 sputter coating system) from $\text{Cu}_6\text{PS}_5\text{Br}$ target (30 mm in Dia.) in radiofrequency Ar discharges. The plasma source power density was fixed at 2000 W yielding the deposition rate of approximately 1.5 nm/min. Target pulsed DC power was fixed at 70 W. Substrates were placed in parallel above the target at the distance 180 mm without additional heating. All depositions were carried out at a floating plasma potential. The base pressure in the chamber was below 7×10^{-4} Pa and the total working gas pressure during deposition was kept at 0.65 Pa.

Structural studies were performed using XRD and SEM techniques (Lyra 3 TESCAN), energy-dispersive X-ray spectroscopy (Bruker XFlash 6) was used to ensure the thin film chemical composition. Electrical resistance of $\text{Cu}_6\text{PS}_5\text{Br}$ -based thin film was measured using the four-contact method in lab-scale measurement system in the temperature interval $T = 4.5 \dots 300$ K. Spectroscopic ellipsometer J.A. Woollam M-2000V was used for measuring the optical constants.

3. Results and discussion

Structural studies were carried out using X-ray diffraction and SEM techniques (Figs. 1 and 2). The diffraction pattern shows the film to be amorphous with some crystalline inclusions, while the diffraction pattern of target was similar to that of $\text{Cu}_6\text{PS}_5\text{Br}$ single crystal (Fig. 1). SEM studies show that the obtained films represent a periodical quasi-two-dimensional system of nanoscaled pillars 100 nm in diameter 1 μm high with distance 10 to 100 nm between them (Fig. 2). On the whole this system is similar to the “forest” with roots strongly attached to substrate surface, and crowns forming bumpy surface of the film (Fig. 2). EDX measurements were used to determine the thin film chemical composition (chemical formula calculated from EDX measurements is $\text{Cu}_{6.35}\text{P}_{1.77}\text{S}_{4.72}\text{Br}_{0.15}$). Thus, films obtained using HiTUS technique appeared to be non-stoichiometric by their chemical composition, enriched with Cu and P atoms and depleted with S and Br atoms, with the sufficiently low Br content.

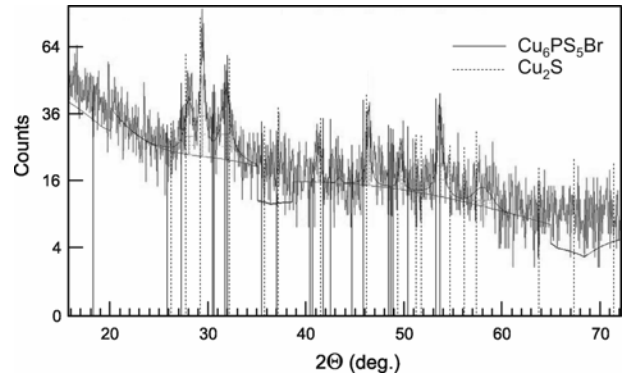


Fig. 1. XRD spectrum of $\text{Cu}_{6.35}\text{P}_{1.77}\text{S}_{4.72}\text{Br}_{0.15}$ thin film.

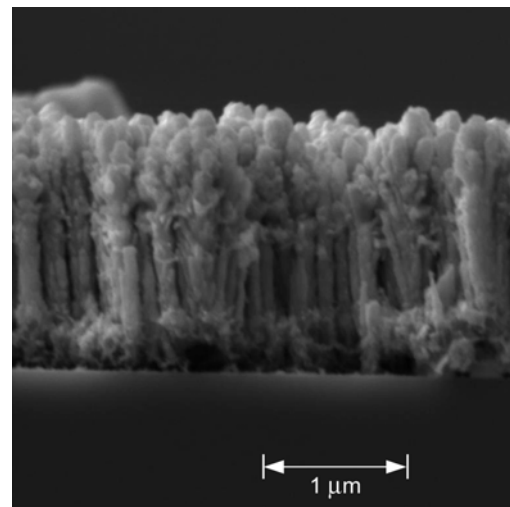


Fig. 2. SEM-image of $\text{Cu}_{6.35}\text{P}_{1.77}\text{S}_{4.72}\text{Br}_{0.15}$ thin film.

The electrical conductivity value for $\text{Cu}_{6.35}\text{P}_{1.77}\text{S}_{4.72}\text{Br}_{0.15}$ thin film at $T = 300$ K equals 4.0×10^{-4} S/m, while at $T = 4.5$ K it equals 6.6×10^{-6} S/m. It should be noted that the electrical conductivity value for $\text{Cu}_6\text{PS}_5\text{Br}$ single crystal at $T = 300$ K equals 1.2×10^{-3} S/m. It is shown that the temperature dependence of electrical conductivity for $\text{Cu}_{6.35}\text{P}_{1.77}\text{S}_{4.72}\text{Br}_{0.15}$ thin film has three regions with different activation energies (Fig. 3).

The dispersion dependences of the refractive index n and extinction coefficient k for the $\text{Cu}_{6.35}\text{P}_{1.77}\text{S}_{4.72}\text{Br}_{0.15}$ thin film were obtained from the spectral-ellipsometric measurements within the spectral range 0.35 to 1.0 μm (Fig. 4). Thus, the refractive index at $\lambda = 1$ μm for $\text{Cu}_{6.35}\text{P}_{1.77}\text{S}_{4.72}\text{Br}_{0.15}$ thin film equals 2.362, while for $\text{Cu}_6\text{PS}_5\text{Br}$ single crystal it equals 2.582. The slight dispersion of the refractive index is observed in the transparency region while it increases when approaching to the optical absorption edge region. The anomalous refractive index dispersion is observed in the region of significant increase of the extinction coefficient.

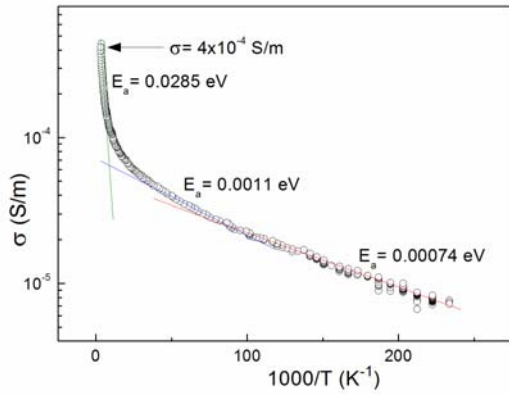


Fig. 3. Temperature dependence of the electrical conductivity for $\text{Cu}_{6.35}\text{P}_{1.77}\text{S}_{4.72}\text{Br}_{0.15}$ thin film.

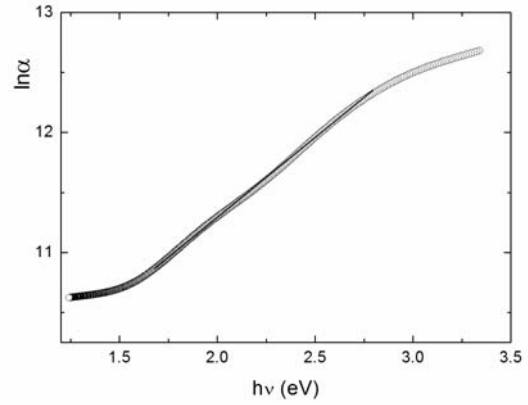


Fig. 5. Spectral dependence of the absorption coefficient for $\text{Cu}_{6.35}\text{P}_{1.77}\text{S}_{4.72}\text{Br}_{0.15}$ thin film.

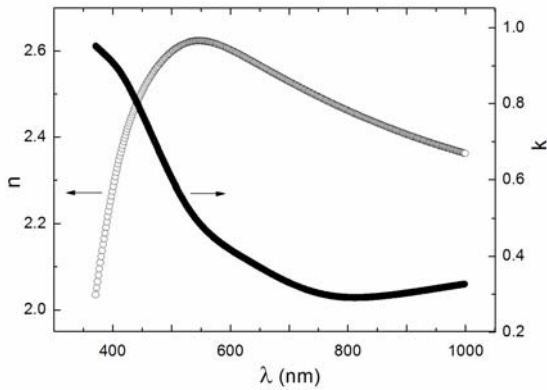


Fig. 4. Spectral dependences of the refractive index and extinction coefficient for $\text{Cu}_{6.35}\text{P}_{1.77}\text{S}_{4.72}\text{Br}_{0.15}$ thin film.

Table. Optical parameters of $\text{Cu}_6\text{PS}_5\text{Br}$ single crystal and $\text{Cu}_{6.35}\text{P}_{1.77}\text{S}_{4.72}\text{Br}_{0.15}$ thin film.

Material	$\text{Cu}_6\text{PS}_5\text{Br}$ crystal	$\text{Cu}_{6.35}\text{P}_{1.77}\text{S}_{4.72}\text{Br}_{0.15}$ thin film
n	2.582	2.362
E_g^α (eV)	2.298	2.682
E_U (meV)	28.1	758

The spectral dependence of the absorption coefficient α which is obtained as $\alpha = 4\pi k/\lambda$, was analyzed in the exponential region for $\text{Cu}_{6.35}\text{P}_{1.77}\text{S}_{4.72}\text{Br}_{0.15}$ thin film (Fig. 5). It is shown that the temperature behaviour of absorption spectrum in the exponential region is described by the well-known Urbach rule [10]

$$\alpha(h\nu, T) = \alpha_0 \cdot \exp\left[\frac{h\nu - E_0}{E_U(T)}\right], \quad (1)$$

where E_U is the Urbach energy (the energy width of the exponential absorption edge), α_0 and E_0 are the convergence point coordinates of the Urbach bundle. In the range of the exponential behaviour of the optical absorption for their spectral characterisation we use such parameter as the energy position of an exponential absorption edge E_g^α at a fixed absorption coefficient α .

In our case, we used the E_g^α values taken at $\alpha = 2 \times 10^5 \text{ cm}^{-1}$ for characterization of the absorption edge spectral position in $\text{Cu}_{6.35}\text{P}_{1.77}\text{S}_{4.72}\text{Br}_{0.15}$ thin film (Table). In Table, we also presents E_g^α at $\alpha = 10^3 \text{ cm}^{-1}$ for $\text{Cu}_6\text{PS}_5\text{Br}$ single crystal.

It should be noted that the essential characteristic of the absorption edge spectrum of the thin film under investigation is very lengthy Urbach tail, which results in the high value of Urbach energy E_U (Table). Thus, the Urbach energy E_U in $\text{Cu}_{6.35}\text{P}_{1.77}\text{S}_{4.72}\text{Br}_{0.15}$ thin film is 758 meV, while in the $\text{Cu}_6\text{PS}_5\text{Br}$ single crystal it equals 28.1 meV. In Ref. [11] it was shown that temperature and structural disordering affects Urbach absorption edge shape, *i.e.*, the Urbach energy E_U is described by the equation

$$E_U = (E_U)_T + (E_U)_X = (E_U)_T + (E_U)_{X, stat} + (E_U)_{X, dyn}, \quad (2)$$

where $(E_U)_T$ and $(E_U)_X$ are the contributions of temperature-related and structural disordering to E_U , respectively; $(E_U)_{X, stat}$ and $(E_U)_{X, dyn}$ are the contributions of static structural disordering and dynamic structural disordering to $(E_U)_X$, respectively.

The temperature-related types of disordering consist from the temperature disordering caused by thermal lattice vibrations and dynamic structural disordering related with availability of mobile ions in the superionic

conductors [12]. The static structural disordering in $\text{Cu}_{6.35}\text{P}_{1.77}\text{S}_{4.72}\text{Br}_{0.15}$ thin film is caused by the following factors: (1) the absence of long-range order in the atomic arrangement and chemical bond breakdown; (2) lower density of the atomic structure packing due to the presence of pores; (3) the transition from the three-dimensional bulk structure to the two-dimensional planar one. Besides, the $(E_U)_{X,stat}$ value in $\text{Cu}_{6.35}\text{P}_{1.77}\text{S}_{4.72}\text{Br}_{0.15}$ thin film may be additionally increased due to the structural imperfectness related to the high concentration of disordered copper vacancies and the dynamic structural disordering $(E_U)_{X,dyn}$ caused by the intense motion of mobile copper ions, participating in ion transport, and which is responsible for the ionic conductivity in crystalline $\text{Cu}_6\text{PS}_5\text{Br}$ and Cu_2S inclusions as well as due to their non-uniform distribution in this amorphous matrix.

4. Conclusions

$\text{Cu}_{6.35}\text{P}_{1.77}\text{S}_{4.72}\text{Br}_{0.15}$ thin film was deposited by the high target utilization sputtering onto *c*-cut sapphire substrates. Temperature behaviour of the electrical conductivity for as-deposited $\text{Cu}_{6.35}\text{P}_{1.77}\text{S}_{4.72}\text{Br}_{0.15}$ thin film was investigated within the temperature interval 4.5...300 K. At 300 K, the electrical conductivity value equals 4.0×10^{-4} S/m, while the temperature dependence of the electrical conductivity has three regions with different activation energies, which is caused by the presence of crystalline inclusions in the amorphous matrix. The spectral dependences of refractive index and extinction coefficient for $\text{Cu}_{6.35}\text{P}_{1.77}\text{S}_{4.72}\text{Br}_{0.15}$ thin film were obtained from ellipsometric measurements. The energy position of absorption edge and the Urbach energy were determined in the range of exponential behavior of the optical absorption edge. The high length of the Urbach tail ($E_U = 758$ meV) is indicative of the significant influence of disordering processes in non-stoichiometric $\text{Cu}_{6.35}\text{P}_{1.77}\text{S}_{4.72}\text{Br}_{0.15}$ thin film. At transition from crystalline $\text{Cu}_6\text{PS}_5\text{Br}$ to amorphous $\text{Cu}_{6.35}\text{P}_{1.77}\text{S}_{4.72}\text{Br}_{0.15}$ thin film, the refractive index decreases.

Acknowledgements

Mykhailo Kutsyk (contract number 51602011) is strongly grateful to the International Visegrad Fund scholarship for funding the project.

References

1. W.F. Kuhs, R. Nitsche, K. Scheunemann, The crystal structure of $\text{Cu}_6\text{PS}_5\text{Br}$, a new superionic conductor // *Acta Cryst.* **B34**, p. 64-70 (1978).
2. R.B. Beeken, J.J. Garbe, N.R. Petersen, Cation mobility in the $\text{Cu}_6\text{PS}_5\text{X}$ ($\text{X} = \text{Cl}, \text{Br}, \text{I}$) argyrodites // *J. Phys. Chem. Solids*, **64**, p. 1261-1264 (2003).
3. T. Nilges, A. Pfitzner, A structural differentiation of quaternary copper argyrodites: Structure – property relations of high temperature ion conductors // *Z. Kristallogr.* **220**, p. 281-294 (2005).
4. A. Haznar, A. Pietraszko, I.P. Studenyak, X-ray study of the superionic phase transition in $\text{Cu}_6\text{PS}_5\text{Br}$ // *Solid State Ionics*, **119**, p. 31-36 (1999).
5. I.P. Studenyak, Gy.S. Kovacs, A.F. Orliukas, E.T. Kovacs, Temperature variations of dielectric and optical properties in $\text{Cu}_6\text{PS}(\text{Se})_3\text{Hal}$ superionics and ferroelastics at phase transitions // *Izvestia Akademii Nauk: Ser. Phys.* **56**, pp. 86-93 (1992).
6. S. Fiechter, E. Gmelin, Thermochemical data of argyrodite-type ionic conductors: $\text{Cu}_6\text{PS}_5\text{Hal}$ ($\text{Hal} = \text{Cl}, \text{Br}, \text{I}$) // *Thermochimica Acta*, **85**, p. 155-158 (1985).
7. V. Samulionis, V. Valevičius, I.P. Studenyak, D.S. Kovač, Acoustic properties of superionic ferroelastic $\text{Cu}_6\text{PS}_5\text{I}$ and $\text{Cu}_6\text{PS}_5\text{Br}$ crystals // *Ultragarsas*, **25**, p.129-136 (1993).
8. V. Samulionis, J. Banys, Y. Vysochanskii, I. Studenyak, Investigation of ultrasonic and acousto-electric properties of ferroelectric-semiconductor crystals // *Ferroelectrics*, **336**, p. 29-38 (2006).
9. I.P. Studenyak, M. Kranjčec, Gy.Sh. Kovacs, V.V. Panko, Yu.M. Azhnyuk, I.D. Desnica, O.M. Borets, Yu.V. Voroshilov, Fundamental optical absorption edge and exciton-phonon interaction in of $\text{Cu}_6\text{PS}_5\text{Br}$ superionic ferroelastic // *Mat. Sci. Engin.* **B52**, p. 202-207 (1998).
10. F. Urbach, The long-wavelength edge of photographic sensitivity and of the electronic absorption of solids // *Phys. Rev.* **92**, p. 1324-1326 (1953).
11. G.D. Cody, T. Tiedje, B. Abeles, B. Brooks, Y. Goldstein, Disorder and the optical-absorption edge of hydrogenated amorphous silicon // *Phys. Rev. Lett.* **47**, p. 1480-1483 (1981).
12. I.P. Studenyak, M. Kranjčec, M.V. Kurik, Urbach rule and disordering processes in $\text{Cu}_6\text{P}(\text{S}_{1-x}\text{Se}_x)_5\text{Br}_{1-y}\text{I}_y$ superionic conductors // *J. Phys. Chem. Solids*, **67**, p. 807-817 (2006).